Spatial Encoding without Gradient Coils Using Field Perturbations from Susceptibility Markers

H. Karimi[1], and C. H. Cunningham[1,2]
[1]Medical Biophysics, University of Toronto, Toronto, ON, Canada, [2]Imaging Research, Sunnybrook Health Sciences Centre, Toronto, ON, Canada

Introduction: In conventional MRI systems, the gradient fields that encode the spatial information are stationary relative to any physiologic movements. In this abstract we propose a novel MR endoscope system [1] based on spatial encoding using the field perturbations around susceptibility markers instead of conventional gradients. This gives the advantage that the frame of reference for the spatial-encoding fields moves with the local tissue displacement. Fig.1 depicts a scaled-up prototype of the proposed device and field perturbation in the main magnetic field. To image with the device, a hard RF pulse is transmitted to excite all the magnetization and FID will be recorded for several ms. Then the device will be rotated by a certain angle and the above procedure is repeated for the new angle. Once all the signals are recorded for sufficient number of angles, a non-Fourier reconstruction process is applied to reconstruct the image at the tip of the catheter. Numerical phantom studies were conducted to assess the feasibility of the proposed method and a prototype device was constructed to demonstrate proof-of-concept using real data.

Theory: When exposed to a magnetic field paramagnetic materials become magnetized with the orientation of that magnetization in the same orientation as the field, and diamagnetic materials become magnetized in the opposite direction [2]. With sub-elements as depicted in Fig. 1(a), the magnetic fields emanating from each of markers will be spatially non-homogeneous, with a magnetic field distribution as depicted in Fig. 1(b). The resulting magnetic field disturbances will move around as the device is rotated. By acquiring MRI data with the sub-elements in a sequence of configurations, giving a sequence of different magnetic-field conditions, sufficient information can be gathered to reconstruct an MR image of the material in the immediate vicinity of the device tip. Let $\Delta B(\bar{x},\theta)$ be the spatially varying magnetic field emanating from the device, as depicted in Fig. 1(c) (with $\theta = 45°$), then a good numerical approximation of $s(\theta_i)$ at time τ_j is given by the following matrix multiplication (Eq.1). For the entire set of angles, the encoding can be written in matrix form as in Eq. 2. By taking the pseudo-inverse of the encoding matrix (E) in Eq. 2, as shown in Eq. 3, it is possible to reconstruct an image at vicinity of the catheter tip.

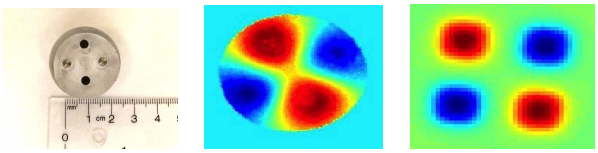

(a) (b) (c)

Fig. 1: (a) the device with 2 titanium and 2 graphite markers (b) Measured frequency shift pattern induced by the device. (c) Simulated frequency shift pattern. Red in the colormap is +60 Hz and blue is -30 Hz

$$(1)\quad s(\theta_i,\tau_j) = \left[e^{i\gamma\Delta B(\bar{x}_1,\theta_i)\tau_j} \quad e^{i\gamma\Delta B(\bar{x}_2,\theta_i)\tau_j} \quad \cdots \quad e^{i\gamma\Delta B(\bar{x}_n,\theta_i)\tau_j} \right] \begin{pmatrix} \rho(\bar{x}_1)\Delta V(\bar{x}_1) \\ \rho(\bar{x}_2)\Delta V(\bar{x}_2) \\ \vdots \\ \rho(\bar{x}_n)\Delta V(\bar{x}_n) \end{pmatrix}$$

$$(2)\quad s = E\rho \qquad (3)\quad \tilde{m} = E^{+}s$$

Methods: To validate the method, we performed simulations and phantom experiments using a prototype device. A numerical phantom study was performed using the simulated phase pattern resulting from paramagnetic and diamagnetic markers with susceptibility differences equal to 200 and -200 ppm as depicted in Fig. 1(c). The encoding matrix was computed using this simulated phase pattern. Then, simulated signals were computed using the phase pattern and a Shepp-Logan numerical phantom, and Eq. 3 was used to compute $\tilde{m}$. For further validation of the method, a scaled prototype of the device was constructed with titanium and graphite markers with the volume magnetic susceptibilities (SI) equal to 171 ppm and -150 ppm, respectively, as depicted in Fig. 1(a). We acquired the phase map using gradient echo sequence (FOV=6cm, TR=33ms, FA=90, 192x192) for two echo times equal to 10ms and 15ms as depicted in Fig. 1(b), and used this measured phase map to compute the encoding matrix. Signals encoded by the device were acquired using a pulse sequence consisting of a 250 μs hard pulse and a 64 ms sampling window (the conventional gradients were not used). Data were acquired with TR=12s to allow time to manually rotate the device by 10° steps between each TR. The other parameters were TE=256 μs, FA=30, FOV=4.0, BW=0.5KHz and 256 samples in read-out direction.

Results and Discussion: The results from the numerical phantom study are shown in Fig. 2, with Fig. 2(b) showing the image reconstructed with Eq. 3. This simulation also showed that the reconstruction will not be affected significantly if the angle of device with respect to B_0 changes by +/- 15° (results not shown). The method was further validated using real signal from a phantom containing holes with different sizes as shown in Fig. 3(a) (GRE, TE=6ms, TR=20ms, FA=30, 128x128). The image of the same phantom is reconstructed using the new method is shown in Fig. 3(b). The quality of this image could likely be improved by using a larger number of angles in the data acquisition, which was not possible with the rudimentary prototype used here. Also, in this proof-of-concept experiment the only signal source was the small holes filled with water in the phantom, which were purposely positioned within the region of support dictated by the phase pattern. This is not realistic, and implementation of this encoding method on a real endoscope will require some means to restrict the signal region, either by using a small receiver coil on the device or employing off-resonance excitation to restrict the excited region. Based on the simulations, the effective field-of-view in front of the device is $r/2$ (r = radius of the device) which enables the acquisition of forward-view, cross-sectional images at the device tip.

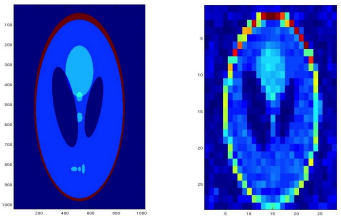

(a) (b)

Fig. 2: (a) Numerical Phantom image (1024×1024 pixels) (b) Reconstructed image (28×28 pixels)

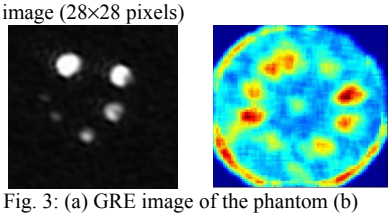

Fig. 3: (a) GRE image of the phantom (b) Image reconstructed using the new method.

Conclusions: A novel MR imaging method using the field perturbations around susceptibility markers as spatial-encoding gradients was proposed. Numerical experiments were performed to explore the issues surrounding the proposed reconstruction process, and data from phantom experiments were reconstructed to show proof-of-concept. Future directions involve developing a fully automated rotating device and a real-time reconstruction process, and eventually testing a device *in vivo*.

References: [1] Sathyanarayana and Bottomley, Med. Phys 36 p. 908 2009 [2] Schenck J. *et al*, Med. Phys. 23, 1996